PARTIAL REMOVAL OF CORRELATED NOISE IN THERMAL IMAGERY

Christoph C. Borel, Bradly J. Cooke and Bryan E. Laubscher
NIS-Division, Mailstop C323, Los Alamos National Laboratory
Los Alamos, NM 87545, USA
cborel@lanl.gov

ABSTRACT

Correlated noise occurs in many imaging systems such as scanners and push-broom imagers. The sources of correlated noise can be from the detectors, pre-amplifiers and sampling circuits. Correlated noise appears as streaking along the scan direction of a scanner or in the along track direction of a push-broom imager. We have developed algorithms to simulate correlated noise and pre-filter to reduce the amount of streaking while not destroying the scene content.

The pre-filter in the Fourier domain consists of the product of two filters. One filter models the correlated noise spectrum, the other is a windowing function e.g. Gaussian or Hanning window with variable width to block high frequency noise away from the origin of the Fourier Transform of the image data. We have optimized the filter parameters for various scenes and find improvements of the RMS error of the original minus the pre-filtered noisy image.

Keywords: 1/f Noise, TDI, Image Quality, Electro-Optics, System Simulation

1 Introduction

Airborne multi-spectral scanners and push broom systems often contain substantial amounts of correlated noise leading to striping visible to an observer. In the past striping has been removed using Fourier analysis techniques, e.g. wedge block filters have been used to improve the qualitative appearance of imagery (Lillesand and Kiefer, 1994). When Fourier analysis was deemed too computationally expensive, simpler spatial filtering methods have been developed (Crippen, 1989).

We have developed a method to partially remove correlated noise for a trade-off study. The goal was to compute if and how much correlated noise could be tolerated in a multi-spectral system capable of imaging in the MWIR and LWIR. The investigated algorithm uses 5 or more images for nadir and off-nadir (30^o and 60^o) and is able to determine sea surface temperatures quite accurately under many atmospheric conditions (Tornow, Borel and Powers, 1994).

Various schemes were investigated for a practical system, e.g. how to subtract linear trends of the correlated noise from the image and the improvement gained by applying the method to various time-delayed integration schemes. To improve radiometric accuracy and ameliorate blurring from the telescope and motion we investigated several image restoration methods such as "Iterative Wiener Filtering" (IWF), "Maximum Entropy Method" (MEM), "Maximum Residual Likelihood" (MRL), etc (see Lim, 1990). The MEM and MRL methods iterate

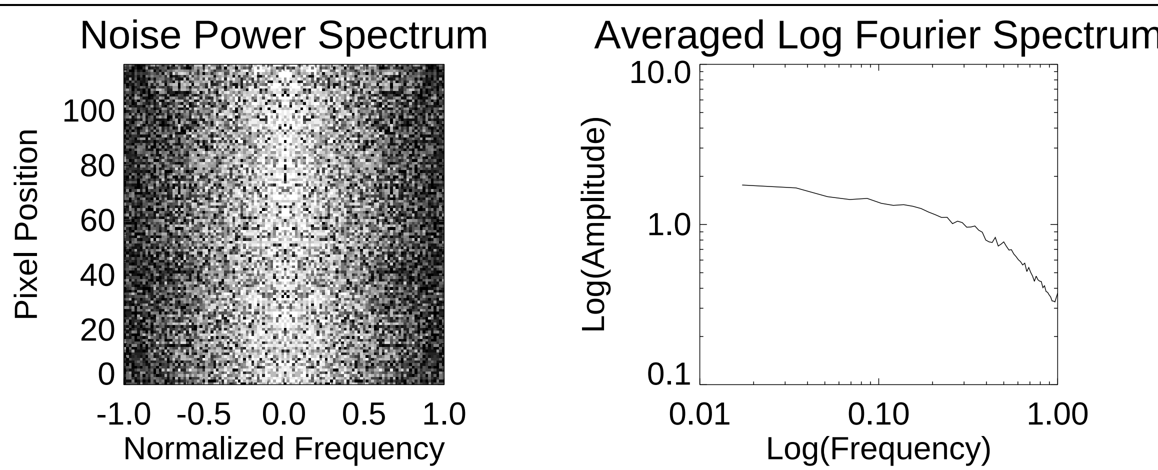

Figure 1: Measured 1/f noise of a MCT camera

until the residual image appears like white Gaussian noise. In order to use MEM and MRL for data which contains correlated noise we had to think of a method to reduce the correlated noise first. We investigated the effect of the pre-filtering on image quality and on the multi-spectral water temperature retrieval algorithm. For scenes with high spatial content the pre-filtering and subsequent image restoration improved the "Root Mean Square Error" (RMSE) by about 1 K.

2 Source of Correlated Noise in Imaging Systems

Correlated noise occurs in many imaging systems such as scanners and push-broom imagers. The sources of correlated noise can be from the detectors, pre-amplifiers and sampling circuits. In Fig. 1 we show the noise spectrum from a typical MCT long wave camera (Inframetrics 600 MCT). The camera was cooled with liquid nitrogen and the lens cover was left on the camera during the measurements. The line and frame integration mode was disabled. One frame was grabbed and saved using the IR imaging software package on floppy disk for further processing. The power spectrum shows that larger amplitudes (light gray level) occur for low frequencies than for higher frequencies. A linear fall-off in a log(frequency)-log(amplitude) plot indicates a power-law correlated noise f^{α} where the slope α ranges typically between -0.25 and -2 (e.g. Keshner (1982) and Hooge (1976)), with true 1/f noise having a slope of $\alpha = -1$. In the case of the present data there seems to be the addition of two different correlated noise sources - a case that can occur in practice.

3 Modeling of Correlated Noise for an Infrared Imager

Correlated noise can be modeled by feeding an uncorrelated noise signal (white noise) in a filter. The order of the filter determines the frequency response (e.g. $N \times 20$ db/decade for a filter of N-th order). In a digital simulation a pseudo random generator was used to generate a signal $s_1(t_k)$ for $x = 1, \ldots, N_x$ samples. The "Fast Fourier Transform " (FFT) of $s_1(t_k)$ is $S_1(f_x)$ and the filter response function is given by $f_(t_k)$ and it's FFT is $F(f_x)$. It can be shown that the output signal of the filter is given by (Lim, 1990) :

$$s_2(t_k) = s_1(t_k) \bigotimes f(t_k) = FFT^{-1}[S_1(f_x)F(f_x)], \quad x = 1, \ldots, N_x \tag{1}$$

where $\otimes$ is a symbol for the discrete convolution. Note that the correlated noise can be produced either by digital filtering which implements the discrete convolution or by the FFT method. We have selected to use the Fourier transform method to simulate the noise signal for an imaging system:

$$\begin{aligned} N_{noise}(x,y) &= N_{uncor}(x,y) + N_{cor}(x,y;\alpha) \\ &= \frac{R_1(x,y)}{STDEV(R_1(x,y))}\frac{1}{SNR_{uncor}} + FFT^{-1}\left[FFT\left[\frac{R_2(x,y)}{STDEV(R_2(x,y))}\frac{1}{SNR_{cor}}\right] f_x^{\alpha}\right], \end{aligned} \quad (2)$$

where R_1 and R_2 are white Gaussian random signals and $STDEV$ denotes the standard deviation. For 1/f noise we have $\alpha = -1$.

4 Algorithm to Partially Remove Correlated Noise

We have developed algorithms to generate correlated noise and pre-filter it to reduce the amount of streaking while minimizing changes of the scene content.

The pre-filter we computed is useful for a scanner and also push-broom mode of operation. Noise in a 2-D frame imager could be reduced over successive frames provided that the scene content did not change.

As the line scanner travels along and builds up a 2-D image, a single pixel traces a line along that image. Each pixel (and its subsequent readout electronics) impresses a correlated noise component onto the scene intensity pattern as it scans in the along track direction. The temporal frequency spectrum of the 1/f noise process is thus translated to a spatial signature. In some cases (i.e., large correlated noise situations and/or uniform scenes) the eye can see the intensity pattern impressed onto the image.

Although there may be a correlated coupling between adjacent scanner pixels, our calculations assumed that the only correlation was between subsequent measurements of each single pixel.

The resulting spatial intensity pattern may be analyzed using the Fourier transform of the image. In a simulated scanning imager, all of the correlated noise power falls in the along-track frequency axis. In a simulated push broom imaging system, all of the correlated noise power in the cross-track frequency axis. See the two middle panels of Figure 3.

The filtering process need be carried out only on the frequency axis where the correlated noise appears (e.g. f_x in Figure 3). If properly filtered, the inverse transformed image will have much less correlated noise contamination (see bottom panels in Figure 3).

The Gaussian function was chosen as our example filter. Note that almost no filtering was performed near the "origin" (location of zero spatial frequency) as these components determine the average flux level of the entire image and contain scene information. Filtering the region near the origin of the transform image will alter the radiometry of the original image.

The filter we choose has is of the general form:

$$F(f_x, f_y) = 1 - F_1(f_x)F_2(f_y), \quad x = 1, \ldots, N_x;\ y = 1, \ldots, N_y, \quad (3)$$

where $F_2(f_y \neq 0; \alpha) = f_y^{\alpha}$ and $F_2(f_y = 0; \alpha) = -1$ represents a correction of the correlated noise and α is the slope in a Log-Log plot of the noise spectrum. For $\alpha = -1$ we have 1/f noise. In the direction x which is perpendicular to the scan direction y we used:

$$F_1(f_x; \beta, \sigma) = (1-\beta)\exp[-(\frac{f_x}{\sigma})^2] + \beta \quad (4)$$

as a weighting function which preserves spectral components near the origin with a standard deviation of σ and offset β which have to be chosen for a particular scene. Another function we tried was a modified Hanning window function:

$$F_1(f_x;\beta,\gamma) = \left[(\beta-1)\cos\left(\frac{2\pi j}{N_x-1}\right)+\beta\right]^\gamma \tag{5}$$

where β is an offset and γ is an exponent to change the width of the peak. The Hanning window is defined for $\beta = 0.5$ and $\gamma = 1$. The Hamming window is defined for $\beta = 0.54$ and $\gamma = 1$. We will use the Gaussian weighting function for the remainder of the paper for the reasons that the width can be given in pixel units and that due to the central limit theorem the overall system "Optical Transfer Function" (OTF) is often Gaussian. The filter will be denoted by $F_{PRCNF}(f_x, f_y; \alpha, \beta, \sigma)$, where $PRCNF$ stands for the "Partial Removal of Correlated Noise Filter" and $\alpha = -1$.

5 OTF and PSF Degradation Effects

The partial removal of correlated noise degrades the overall "Optical Transfer Function" (OTF) and "Point Spread Function" (PSF) of the optical system, e.g.:

$$\begin{aligned} OTF_{tot}(f_x, f_y) &= OTF_{Atmosphere}(f_x, f_y) OTF_{Telescope}(f_x, f_y) OTF_{Motion}(f_x, f_y)\ldots \\ &\quad OTF_{Pixel}(f_x, f_y) OTF_{Electronics}(f_x, f_y) OTF_{PRCNF}(f_x, f_y; \alpha, \beta, \sigma), \end{aligned} \tag{6}$$

where $PRCNF$ stands for the "Partial Removal of Correlated Noise Filter". Note however that this does not necessarily mean that the effective image content and radiometric accuracy are degraded. In uniform scenes the "striping"effect can be significantly reduced using the PRCNF method. Simultaneously the Root Mean Square Error (RMSE) of the difference between the "original" image (with no noise) and the PRCNF filtered noisy image is dramatically reduced thus leading to better radiometric accuracy. In heterogeneous scenes with high spatial frequencies the use of the PRCNF will blur the image somewhat. In Figure 2 we plot the OTF of the PRCNF with $\alpha = -1,\ \beta = 0.1$ and $\sigma = 0.1 * N_x$.

6 Optimizing Method

Based on imagery from the scene of interest which we assume has not been affected by correlated noise it is possible to optimize the PRCNF parameters β and $sigma$ for the Gaussian weighting function and β and γ for the modified Hanning window. Let $I_{ref}(x, y)$ be a reference image of the scene of interest with no correlated noise (e.g. taken by a MWIR imager). Let $N_{noise}(x, y) = N_{uncor}(x, y) + N_{cor}(x, y; \alpha)$ (eq. (2))be a noise image taken by the LWIR sensor without a scene (e.g. closed aperture, blackbody of similar brightness temperature as the scene). The following procedure was used to find the (near) optimum PRCNF and filter the measured image:

1. Let $I_1(x, y) = I_{ref}(x, y) + N_{noise}(x, y)$ be a "simulated" scene with both noises (band limited white and correlated) added and filter it with $F_{PRCNF}(f_x, f_y; \alpha, \beta, \sigma)$ to result in:

$$I_2(x, y) = FFT^{-1}\left[I_1(f_x, f_y) F_{PRCNF}(f_x, f_y; \alpha, \beta, \sigma)\right]$$

2. Compute the RMSE of $(I_2(x, y) - I_{ref}(x, y)$ and select the optimum PRCNF parameters: $\beta_{opt},\ \sigma_{opt}$ when $RMSE(\beta_{opt}, \sigma_{opt}) = Min$

3. Filter the true scene image I_3 which contains similar both kinds of noise similar to the noise image $N_{noise}(x, y)$:

$$I_4(x, y) = FFT^{-1}\left[I_3(f_x, f_y) F_{PRCNF}(f_x, f_y; \beta_{opt}, \sigma_{opt})\right]$$

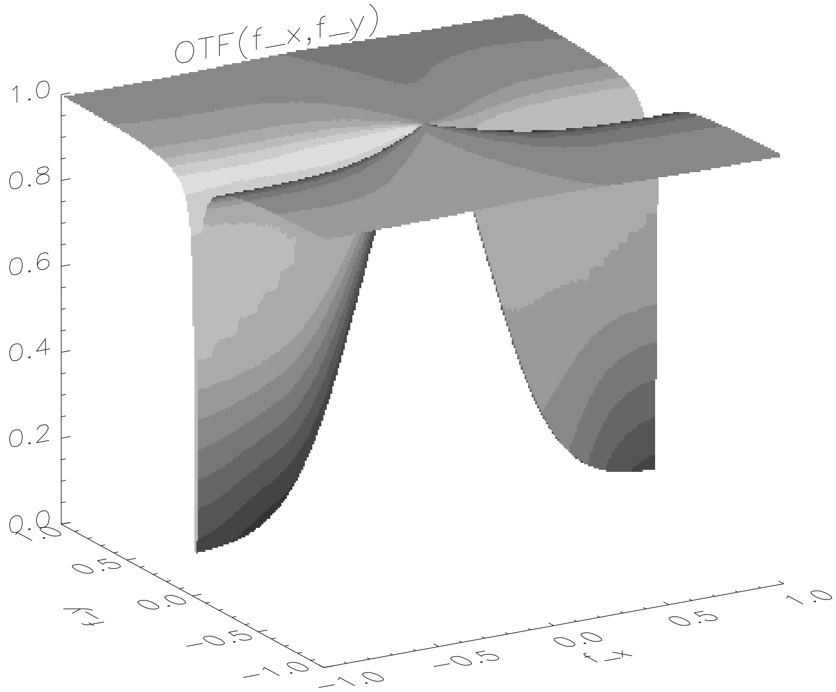

Figure 2: OTF of the "Partial Removal of Correlated Noise Filter"

Note that for highly structured scenes the optimum filter will remove less correlated noise because the scene content would be too much degraded. The striping will be reduced more when the scene has few sharp features, e.g. night time LWIR scenes. We did not attempt to create an adaptive filter which changes the filter parameters according to scene content. The optimization of the proposed filter is graphed in Figure 4 using the following definitions:

$$RMSE1 = RMSE(I_{ref}(x,y) - FFT^{-1}\left[I_{ref}(f_x,f_y)F_{PRCNF}(f_x,f_y;\beta_{opt},\sigma_{opt})\right]$$

$$RMSE2 = RMSE(I_2(x,y) - I_{ref}(x,y))$$

and

$$Ratio_{STDEV} = \frac{STEDEV(I_2(x,y))}{STDEV(I_1(x,y))}.$$

Note we plot $RMSE1$, $RMSE2$ and $Ratio_{STDEV}$ in units of K.

7 Subtracting Linear Trends and Time Delayed Integration

For a scanner it is possible to make a measurement of an internal blackbody before (at time T_a and pixel $y_a = T_a/\Delta T$, where ΔT is the time between samples) and after a scan (at time T_b and pixel y_b). For a push broom sensor a measurement of a constant blackbody source is possible before and after image acquisition. For the push broom case this allows the removal of a linear trend or slope in the signal by:

$$I_{slope}(x,y) = I_1(x,y) - \left[I_1(x,y_a) + \frac{I_1(x,y_b) - I_(x,y_a)}{y_b - y_a}y\right] \tag{7}$$

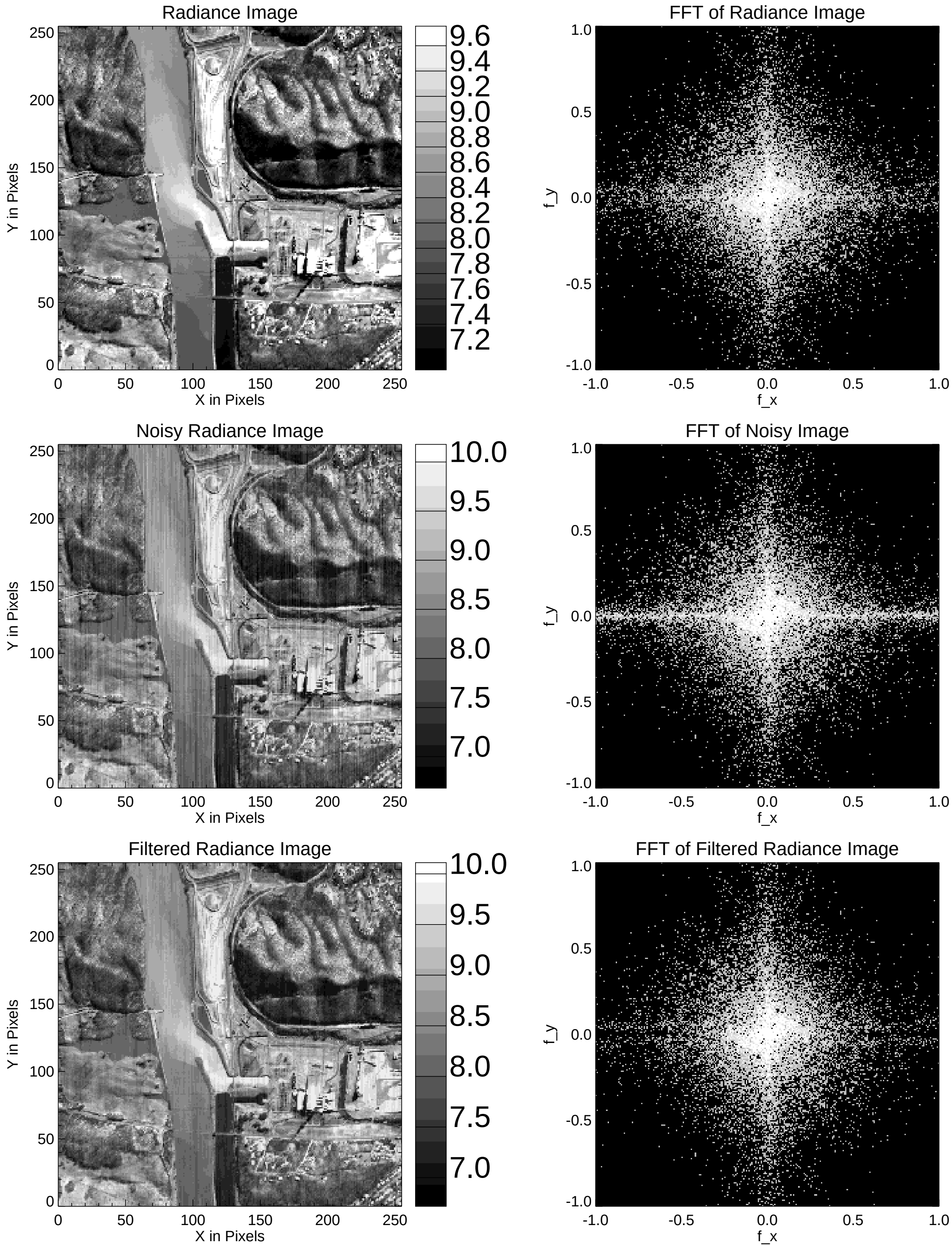

Figure 3: Example of partial removal of correlated noise ($SNR_{cor} = 50$ and $SNR_{uncor} = 500$)

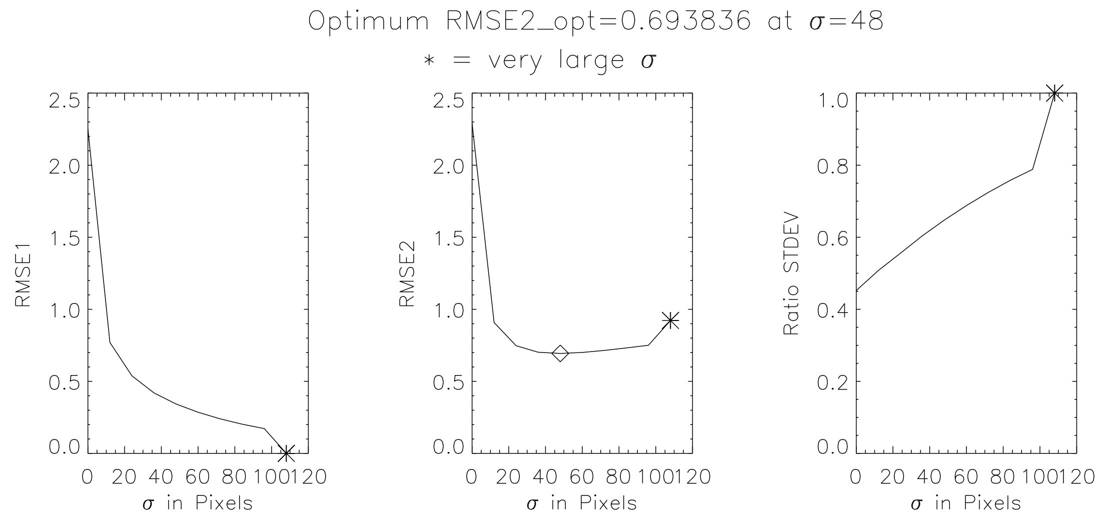

Figure 4: Optimization result for the images shown in Figure 3

An example of linear trend removal is shown in Figure 5. Note that the trend removal reduces the amplitudes of the 1/f noise.

The slope corrected image $I_{slope}(x, y)$ is then filtered using the $PRCNF$ method. The observed improvement in the previous image was surprisingly small (0.6754 vs 0.6938) for the case $y_a = 0$ and $y_b = N_y = 255$.

A scanner was simulated by generating 256 realizations of correlated noise with 256 samples each. Assuming $y_a = 0$ and $y_b = 255$ we computed the ratio:

$$Ratio_{STDEV} = \frac{\sigma(I_{slope})}{\sigma(I_{noise})},$$

for a noise with $SNR_{cor} = 50$ and $SNR_{uncor} = 500$. We found that the mean $Mean(Ratio_{STDEV}) = 0.81$ and the standard deviation $STDEV(Ratio_{STDEV}) = 0.248$, thus an improvement in SNR is obtained when the linear trend is removed. Note however that it possible occasionally that the $Ratio_{STDEV}$ is above unity, e.g. the noise measurements have both similar large magnitudes but the noise mean is close to zero. The slope correction fails if one waits too long before and after image acquisition for the noise measurements (e.g. $T_b - T_a >> N_y \Delta T$).

A better method to improve SNR is achieved by a "Time Delay Integration" (TDI) scheme where we assume to have N_{TDI} independent detector arrays. The improvement in SNR is given by (Holst, 1995):

$$SNR_{TDI} = \sqrt{N_{TDI}} SNR_{detector}.$$

We tested the $PRCNF$ method on the summed images at each TDI step but could not improve the RMSE beyond the simple averaging of samples.

8 Conclusions

A method has been developed which reduces the visually disturbing effect of correlated 1/f noise in long wave thermal imagery while preserving the image resolution and radiometric accuracy. The PRCNF method can be

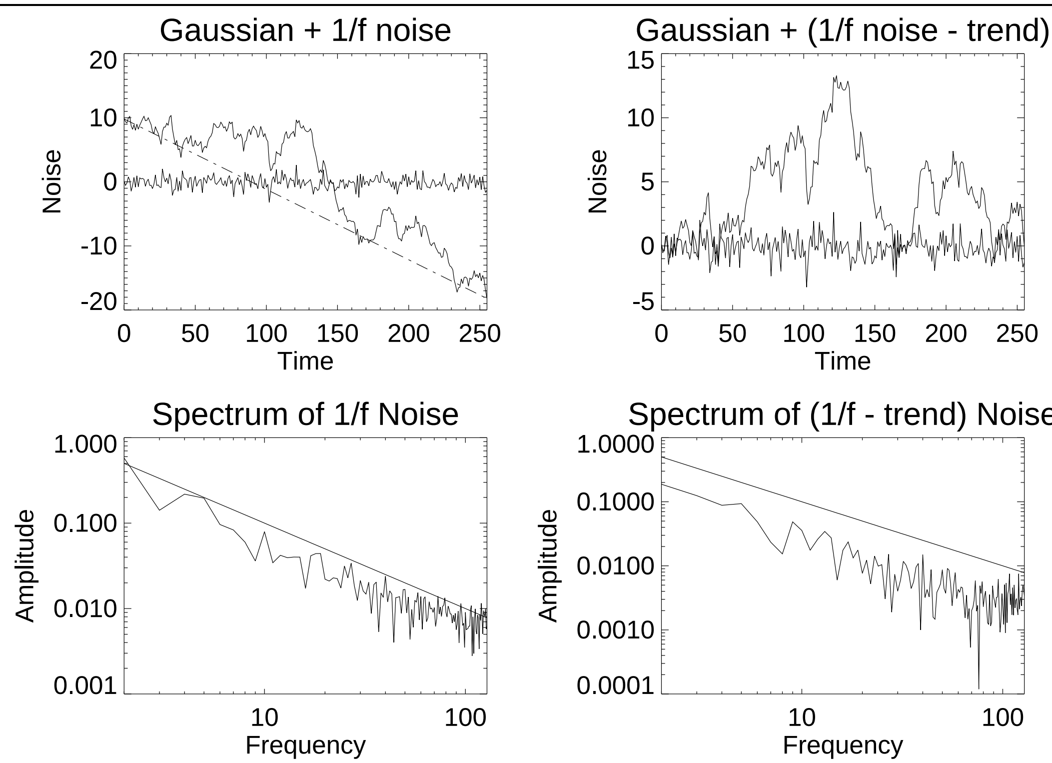

Figure 5: Simulation of linear trend removal.

optimized for a given scene if an almost noise free image in another thermal channel (e.g. MWIR) is available, and a noise image in the channel of interest.

9 References

R.E. Crippen, "A Spatial Filtering Routine for the Cosmetic Removal of Scan-Line Noise from Landsat TM P-Tape Imagery", Photogrammetric Engineering and Remote Sensing, 55:3:327-331, 1989.

F.N. Hooge, "1/f noise", Physica, 83B:14-23, 1976.

G.R. Holst, *Electro-Optical Imaging System Performance*, SPIE Eng. Press and JCD Publishing, 1995.

M.S. Keshner, "1/f noise", Proc. IEEE, 70:3:212-218, 1982.

T.M. Lillesand and R.W. Kiefer, *Remote Sensing and Image Interpretation*, John Wiley & Sons, 1994.

J.S. Lim, *Two-Dimensional Signal and Image Processing*, Prentice Hall, 1990.

C. Tornow, C.C. Borel and B.J. Powers, "Robust Water Temperature Retrieval using Multi-Spectral and Multi-

Angular IR Measurements", IGARSS'94 Conference, August 8-12, 1994.